

Branched Polymer Architecture Formed in Conventional and Living Emulsion Polymerization

Hidetaka TOBITA*

(Received January 14, 2022)

Emulsion polymerization proceeds in a unique locus of polymerization, having confined submicron space with a higher polymer concentration from the beginning of polymerization. Assuming the ideal polymerization kinetics during Interval II in emulsion polymerization, the branched architecture formed by the chain transfer reaction to the polymer is investigated by using a Monte Carlo simulation method, both for the conventional and the living free-radical polymerization (FRP). The conventional FRP leads to form a broad molecular weight distribution (MWD), while the living FRP gives a rather narrow MWD. The expected contraction ratio g of the mean-square radius of gyration Rg^2 of the branched polymer to that of a linear polymer for a given number of branch points k is essentially the same, at least approximately, both for the conventional and the living FRP, irrespective of the reaction condition, and a universal equation is proposed for the g - k relationship. The magnitude of Rg^2 can be represented by using the maximum span length L_{MS} , $Rg^2 = 0.172 L_{MS}$, both for the conventional and the living FRP. Similar relationships, $Rg^2 = a L_{MS}$ with $a = 0.17$ – 0.18 apply to various types of branched polymers, and could be considered as a universal relationship.

Key Words : Branched Polymers, Chain Transfer to Polymer, Emulsion Polymerization, Living Radical Polymerization, Molecular Weight Distribution, Radius of Gyration

1. Introduction

Polymerization is a reaction process in which monomers are converted to polymers, and therefore, the weight fraction of polymer increases just linearly with the monomer conversion x , as shown by the dotted line in Fig. 1 for usual bulk polymerization. On the other hand, the locus of polymerization in emulsion polymerization is the polymer particle, which is schematically shown in Fig. 2. After a short nucleation period, called Interval I, the weight fraction of polymer in the polymer particle is approximately kept constant until the depletion of monomer droplets, due to the monomer transfer from the monomer droplets to the polymer particles. The constant polymer weight fraction period, which leads to a constant polymerization rate period in a typical emulsion polymerization, is called

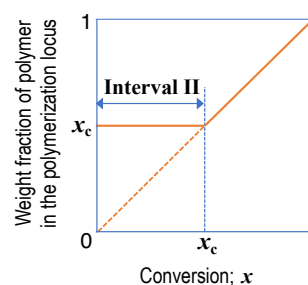


Fig.1 Polymer weight fraction development in the polymerization locus during emulsion (solid line) and bulk polymerization.

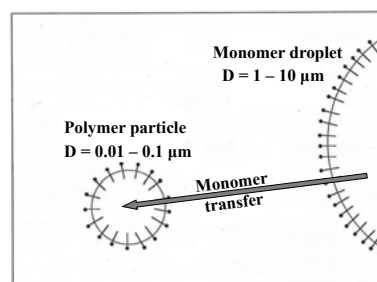


Fig. 2 Illustration of the emulsion polymerization during Interval II.

* Department of Materials Science and Engineering

Interval II. Assuming the nucleation period is small enough, the weight fraction of polymer in the polymer particle changes as shown by the solid line in Fig. 1. In this article, the branched polymer formation due to the chain transfer to polymer is investigated theoretically during Interval II.

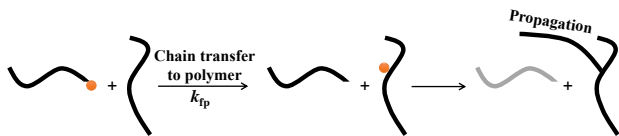


Fig. 3 Schematic representation of the process of chain transfer to polymer in free-radical polymerization (FRP).

Fig. 3 shows the process of chain transfer to polymer, leading to the long-chain branching. The rate R_{fp} of chain transfer to polymer is represented by:

$$R_{fp} = k_{fp}[R^*][M]_0 x_c \quad (1)$$

where k_{fp} is the rate constant for the chain transfer to polymer, $[R^*]$ is the radical concentration, $[M]_0$ is the initial monomer concentration, and x_c is the weight fraction of polymer in the polymer particle, which is equal to the monomer conversion at which the monomer droplets are depleted, as shown in Fig. 1. In usual polymerization in a homogeneous medium, R_{fp} is zero at conversion $x = 0$, because polymer is not present. On the other hand, R_{fp} is large from the beginning in emulsion polymerization. Emulsion polymerization promotes the branching reaction.

The rate R_p of polymerization is given by:

$$R_p = k_p[R^*][M]_0(1-x_c) \quad (2)$$

where k_p is the propagation rate constant.

The branching density ρ is defined as the fraction of units that bear a tri-branch point. The instantaneous branching density is given by the rate ratio of R_{fp} and R_p , which is given by:

$$\rho = \frac{R_{fp}}{R_p} = C_{fp} \frac{x_c}{1-x_c} \quad (3)$$

where C_{fp} ($= k_{fp}/k_p$) is the chain transfer constant to polymer. Equation (3) shows that the branching density is kept constant throughout Interval II, investigated in this article.

Although the branching density of the whole polymer is kept constant, the branching density or the probability of possessing a branch point in a unit in chain is different,

depending on when the unit is incorporated into the polymer chain. The units that are incorporated in the earlier stage of polymerization are subjected to the polymer transfer reaction for a longer period of time, compared with those bound in the later stage of polymerization. The branching density of a unit in chain is a function of the time when the monomer turns into polymer.

The total number n of monomeric units incorporated into polymer in a polymer particle increases with time. Suppose $n = n_p$ at the present time. The expected branching density ρ_{unit} of a unit bound into polymer at $n = n_b$ is given by the following equation.^[1]

$$\rho_{unit}(n_b, n_p) = C_{fp} \frac{x_c}{1-x_c} \ln \left(\frac{n_p}{n_b} \right) \quad \text{for Interval II.} \quad (4)$$

Fig. 4 shows the calculated result of the branching density distribution represented by Eq. (4) at $n_p = 1 \times 10^6$. A large variation in the branching density distribution is an important characteristic of emulsion polymerization, although the average branching density ($= \rho$) is kept constant throughout Interval II.

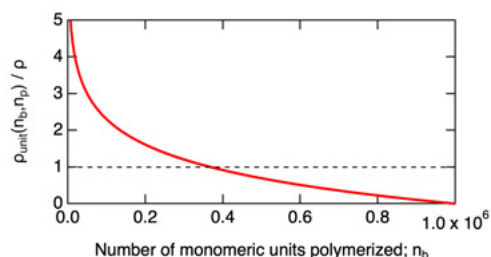


Fig. 4 Branching density distribution ρ_{unit} during Interval II at $n_p = 1 \times 10^6$, calculated from Eq. (4).

When discussing the branched polymer architecture, the primary polymer chain^[2] is a useful concept. The primary polymer chain is a linear chain when all branch points are severed. In the conventional FRP, each primary chain is formed instantaneously, therefore, Fig. 4 shows that the primary chains that are formed in the earlier stage of polymerization possess a larger branching density than those formed in the later stage of polymerization. The variation in the branching density is among the primary chains in the conventional FRP.

On the other hand, in the living FRP, or the reversible-deactivation radical polymerization in the IUPAC terminology,^[3] the variation in the branching density is observed along the sequence of a primary polymer chain. Note that when the growing primary

chain causes the polymer transfer reaction, this primary chain becomes a dead primary chain, while a new growing primary polymer chain is formed from a radical on a backbone chain.

In this article, the statistical properties, such as the molecular weight distribution and the radius of gyration, of the branched polymer molecules formed in the conventional and the living emulsion polymerization are investigated, seeking for newer methods to design and control the branched polymer architecture.

2. Method

The Monte Carlo simulation method to generate the branched polymer architecture of each polymer molecule is described in detail in ref.^[4] As described therein, the number fraction distribution $N_p(r)$ of the primary polymer chains in emulsion polymerization during interval II is typically given by the following most probable distribution.

$$N_p(r) = \frac{1}{\bar{P}_{np}} \exp\left(-\frac{r}{\bar{P}_{np}}\right) \quad (5)$$

where r is the chain length, and \bar{P}_{np} is the number-average chain length of the primary polymer molecules.

For the living FRP, the termination reaction is neglected, and the average number of monomeric units added during a single growth period is set to be 2, as was done earlier.^[4,5]

The statistical analysis is conducted when the number of monomeric units polymerized in a polymer particle reaches $n = 1 \times 10^6$. Assuming that the molecular weight of the monomer is 100, and the density of polymer is 1 g/cm^3 , the diameter of a dried polymer particle at $n = 1 \times 10^6$ is 68 nm, which conforms to a normal emulsion polymerization experiment during Interval II. A large number of polymer particles are simulated to determine statistically valid properties.

3. Results and Discussion

3.1 Calculation Conditions

The systematic analyses are conducted by using the conditions shown in Table 1. C1–C4 are the conventional FRP, and L1–L4 are the living FRP.

The branching probability P_b , which is the probability for a primary polymer chain end to be connected to the

backbone polymer chain is increased from 0.2857 (top: C1, L1) to 0.8333 (bottom: C4, L4).

Table 1. Calculation conditions

Run	\bar{P}_n ¹⁾	ρ ²⁾	\bar{P}_{np} ³⁾	P_b ⁴⁾
C1, L1	200	0.002	142.9	0.2857
C2, L2	500	0.002	250	0.5
C3, L3	1000	0.002	333.3	0.6667
C4, L4	1000	0.005	166.7	0.8333

¹⁾ The number-average chain length of the product polymers.

²⁾ The average branching density of the product polymer. ³⁾ The number-average chain length of the primary polymer chains.

⁴⁾ The probability that the chain end of a primary chain is connected to the backbone chain, named branching probability.

Fig. 5 shows the weight fraction distribution of the primary chains. In the figure, PDI means the polydispersity index, which is the ratio between the weight- and number-average, representing the degree of breadth of the chain length distribution. For the conventional FRP, PDI = 2 for all C1–C4, because the PDI of the most probable distribution is 2.

For the living FRP, the smooth low molecular weight curve represents the primary chains that have experienced chain stoppage through the polymer transfer reaction. In L1, most primary chains do not experience the polymer transfer reaction, which is represented by the sharp high molecular weight peak. On the other hand, most of the primary chains in L4 are subjected to the polymer transfer reaction to form a distribution close to the most probable distribution whose PDI is nearly 2.

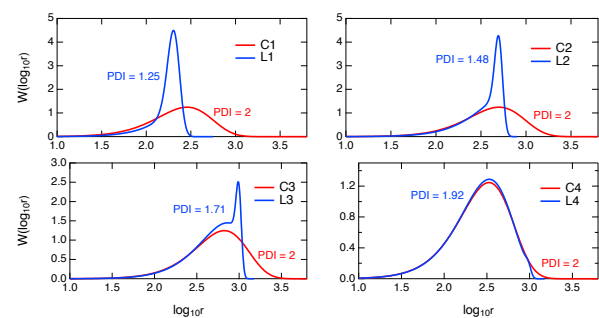


Fig. 5 Primary chain length distribution.

3.2 Molecular Weight Distribution (MWD)

3.2.1 Conventional FRP

Fig. 6 shows the weight fraction distribution of the product branched polymers for the conventional FRP at $n = 1 \times 10^6$. As the branching probability P_b increases, the

distribution becomes broader, and PDI is as large as 109 for C4. The distribution is broader than the random branching of the same primary polymer chains,^[4] and it is shown that the present type of nonrandom distribution of branch points, represented by Eq. (4) and Fig. 4, leads to a broader molecular weight distribution in the conventional FRP.

When P_b is large, as in the cases of C3 and C4, another high molecular weight (MW) peak appears. This high MW peak is formed because of the limitation of the small particle size. In the present simulation, the total number of monomeric units incorporated into polymer molecules in a particle is $n = 1 \times 10^6$, and therefore, it is impossible to form a polymer molecule whose chain length (degree of polymerization) is larger than 1×10^6 . In fact, the polymer molecules in the high MW peak in C4 are the largest polymer molecule in each polymer particle. These polymer molecules want to grow further, but they cannot because of the limitation of the particle size. This type of confined space effect may become important in nonlinear emulsion polymerization.

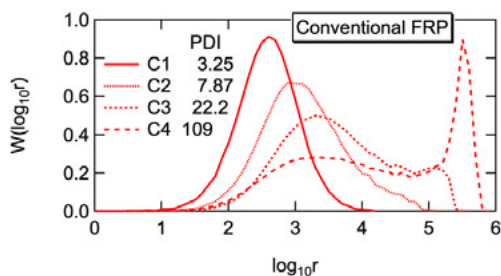


Fig. 6 Weight fraction distribution of the product polymers at $n = 1 \times 10^6$, for the conventional FRP, C1–C4.

Another interesting characteristic of the conventional FRP conducted in a constant polymer/monomer condition is that the MWD of the high MW tail follows the power law, represented by the following weight-based distribution function.^[6,7]

$$W(r) \propto r^{-1/P_b}, \quad (6a)$$

or equivalently, in the number-based functional form:

$$N(r) \propto r^{-(1/P_b+1)}. \quad (6b)$$

Fig. 7 shows the double logarithmic plot of the number fraction distribution $N(r)$ of C1–C4. The power-law distribution represented by Eq. (6b) is confirmed, including the bimodal distributions observed for C3 and C4 shown in Fig. 6. Because the slope is related with P_b , the power-law distribution can be used to determine the

chain transfer constant experimentally.^[7]

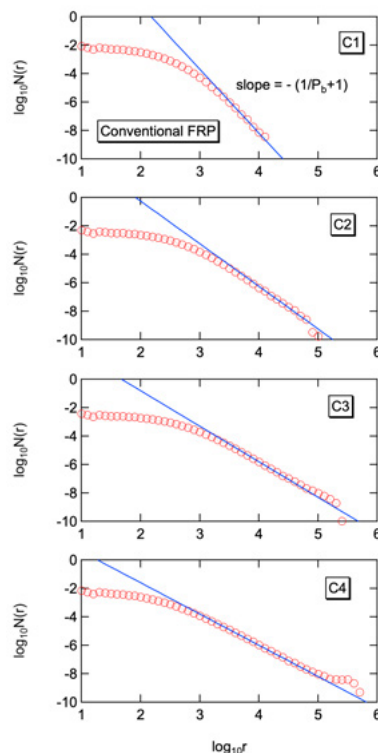


Fig. 7 Double logarithmic plot of the number fraction distribution $N(r)$ of the polymers formed in the conventional FRP, C1–C4.

The red bimodal MWD shown in Fig. 8 is the experimental result reported for the emulsion polymerization of ethylene,^[8] which is known to have a large frequency of branching through chain transfer to polymer. A bimodal MW distribution, as in the case of C4, is observed. When the MWD, $W(\log_{10}M)$ is converted to $W(M)$ and plotted in the double logarithmic form, one obtains the dotted curve, showing a power-law relationship for the important MW region. $P_b = 1/1.23 = 0.813$ leads to give the chain transfer constant C_{fp} that agrees reasonably well with the reported value.^[7]

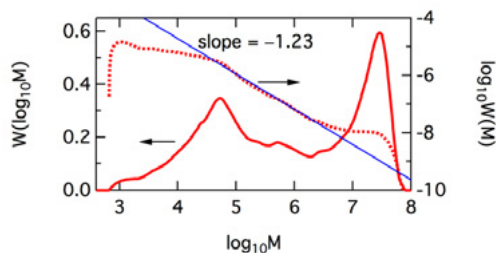


Fig. 8 MWD of the emulsion-polymerized polyethylene, reported in ref.^[8] In the figure, M is the molecular weight, and is related with chain length (degree of polymerization) r by $M = 28 r$.

3.2.2 Living FRP

Fig. 9 shows the simulated weight fraction distribution for L1–L4. Although the branching density ρ is the same as for the corresponding conventional FRP, for example L1 and C1, significant broadening of the MWD, as was observed for the conventional FRP, is not found. In fact, the distribution is narrower than the random branching of the same primary chains.^[4] The polymers with extremely large MW are not formed in the living FRP.

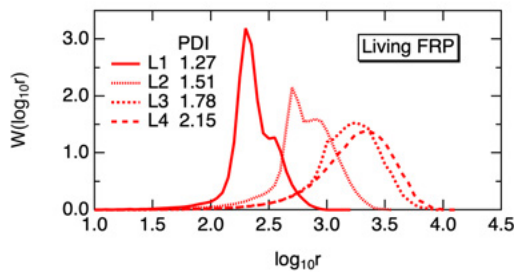


Fig. 9 Weight fraction distribution of the product polymers at $n = 1 \times 10^6$, for the living FRP, L1–L4.

Table 2 shows how the PDI changes with branching. Interestingly, the PDI does not change significantly in the living FRP, which is a notable difference in contrast to the conventional FRP. Note that the primary chain length distribution cannot be determined in a straightforward manner in a usual emulsion polymerization experiment, and all one can obtain is the MWD of the product polymers. It may be difficult to find the existence of branches, judging solely from the product polymer distribution because the PDI values are so small.

Table 2 Polydispersity index (PDI) of the primary chains and the product branched polymers, for L1–L4.

	Primary chains	Product polymers
L1	1.25	1.27
L2	1.48	1.51
L3	1.71	1.78
L4	1.92	2.15

3.3 Radius of Gyration

The mean-square radius of gyration Rg^2 describes the spatial dimension of the polymer. To highlight the effect of branching in polymer, the g -ratio of Rg^2 of the branched polymer to that of a linear polymer is a useful measure.

$$g = \frac{Rg_{\text{Branched}}^2}{Rg_{\text{Linear}}^2}. \quad (7)$$

As a standard branched polymer structure, the Zimm-Stockmayer equation^[9] that describes the random branching of the primary chains with the most probable distribution has been used widely. The expected g -value for the polymer molecules having k branch points is given by:

[Zimm-Stockmayer]

$$g = \left[\left(1 + \frac{k}{7} \right)^{0.5} + \frac{4k}{9\pi} \right]^{-0.5} \quad (8)$$

Note that the branched architecture formed in the present emulsion polymerization system is not random, as shown by the branching density distribution in Fig. 4. For the primary chain length distribution, the most probable distribution applies for the conventional FRP, but not for the living FRP, as shown in Fig. 5.

Fig. 10 shows the g - k relationship for C4. Each red dot represents a pair of values for each polymer molecule, g and k . The blue open circles show the average within the intervals of Δk , representing the expected g -value for a given k .

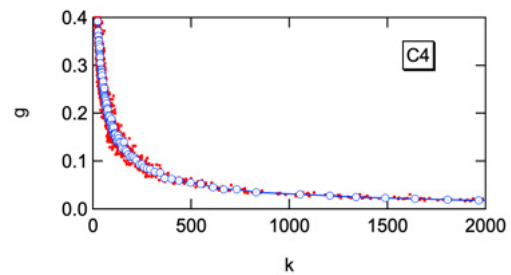


Fig. 10 Relationship between g and k for C4.

Fig. 11 shows the expected g - k relationships for the conventional FRPs. It is interesting to note that the relationships stay nicely on a single universal curve, irrespective of the calculation condition.

The black solid line shows the Zimm-Stockmayer theory, represented by Eq. (8), and the conventional FRP shows smaller g -values, i.e., smaller radius of gyration. Because the primary chains in C1–C4 follow the most probable distribution, which is the same as the assumption used in the Zimm-Stockmayer theory, the difference must come from the nonrandom connection of the primary chains. The compact architecture formed in the conventional FRP, compared with the random branching, could be rationalized, based on the branching

density distribution shown in Fig. 4. In the conventional FRP, each primary chain is formed instantaneously, and the primary chains formed in the earlier stage of polymerization are expected to possess larger values of branching density. These primary chains are likely to bear a large number of branch chains, leading to form a core region, resulting in an overall star-like architecture. This would be the reason for showing smaller g -values.

Incidentally, Eq. (8) represents $g \propto k^{-0.5}$ for the large k region, while the simulation results show $g \propto k^{-0.8}$, as represented by the dotted line in Fig. 11b. This finding will be used to find the universal g - k relationship.

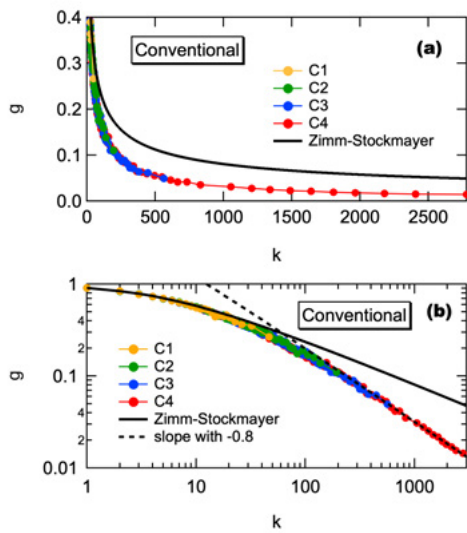


Fig. 11 Relationship between g and k for the conventional FRP, C1–C4. (a) Normal plot. (b) Double logarithmic plot.

Fig. 12 shows the g - k relationships for the living FRPs, L1–L4. A slight increase by the branching probability P_b is observed, however, the difference is rather small, and it could be considered essentially the same g - k relationship for all conditions.

The solid black curve shows the Zimm-Stockmayer theory, and the g - k relationship appears to be close. On the other hand, this seemingly close relationship is just coincidental, because the primary chain length distribution is much different from the most probable distribution, as shown in Fig. 5.

It is already known that the narrower primary chain length distribution leads to a smaller g -value in the random branched polymers.^[10] For the primary chains that follow the Schulz-Zimm distribution, the following equation was proposed.

[Random branch of the Schulz-Zimm chains]

$$g = \left[\left(1 + \frac{k}{5 + \text{PDI}} \right)^{0.5} + \frac{4k}{(1 + 4\text{PDI})\pi} \right]^{-0.5} \quad (9)$$

Note that the Schulz-Zimm distribution, or the Gamma distribution in the mathematical term, is a generalized form of the most probable distribution, and Eq. (9) reduces to Eq. (8) when $\text{PDI} = 2$.

The primary chain length distribution becomes broader in the order from L1 to L4, and therefore, it could be expected that the g -value increases from L1 to L4. However, the obtained g - k relationship is essentially the same, as shown in Fig. 12.

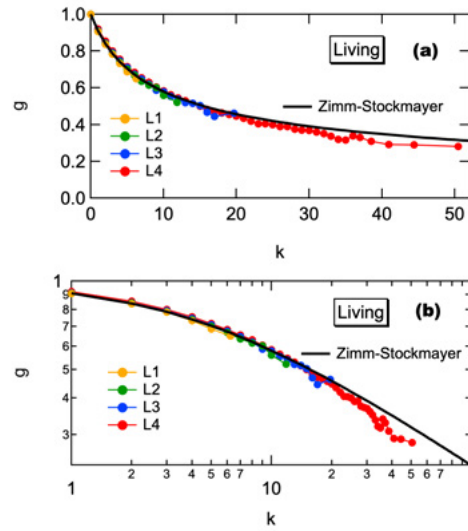


Fig. 12 Relationship between g and k for the living FRP, L1–L4. (a) Normal plot. (b) Double logarithmic plot.

To remove the difference of primary chain length distribution, the g - k relationships for the random branched polymers of L1–L4 conditions shown in Fig. 5 are determined by using the MC simulation. Fig. 13 shows the comparison. When the branching probability P_b is small (L1), the g -value is larger than the corresponding random branch case, but the difference becomes smaller as P_b increases, and the g -value is smaller than the random branch in L4.

Incidentally, the black solid curves for the random branched polymers in Fig. 13 are calculated from Eq. (9), and they agree with the MC simulation results well, even though the primary chain length distribution assumed is different from the Schulz-Zimm distribution. Equation (9) could be used to estimate the g -values of the random branched polymers in general.

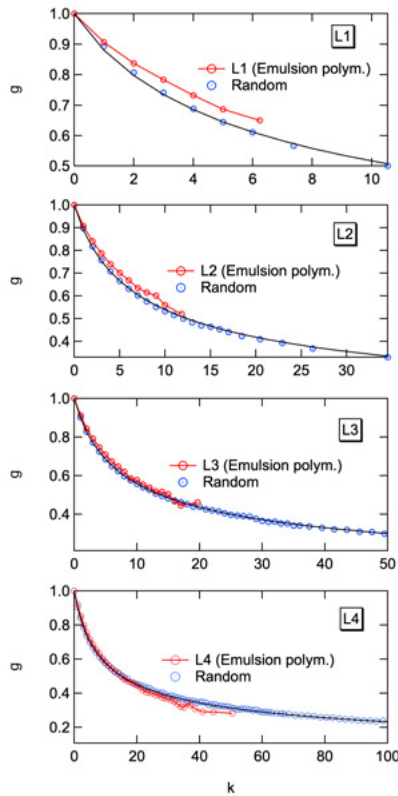


Fig. 13 Comparison of the g - k relationship. The primary chain length distribution is set to be the same for the corresponding cases.

For L4, most primary chains experience the chain stoppage due to the chain transfer reaction, as can be guessed from the primary chain length distribution shown in Fig. 5. In this case, the situation is similar to the conventional FRP. The primary chains formed earlier are expected to possess a larger number of branch chains, and a core region could be formed. It is reasonable to consider that more compact architecture is formed, compared with random branching.

On the other hand, in L1, most primary chains do not experience chain stoppage, and the branching density distribution shown in Fig. 4 is expected to be observed along the sequence of a primary chain. The probability of possessing a branch point is higher for the units located closer to the starting point. If these earlier incorporated units are subjected to the chain transfer reaction at the earlier stage of polymerization, the length of the connected branch chains could be long, because they have enough time for growth. This type of event would introduce a long linear polymer part in the formed branch polymer molecule, which makes the radius of gyration larger. This would be the reason for obtaining a larger g -value, compared with the random branching.

As the branching probability P_b increases, the primary chain length distribution becomes broader, which would make the g -value larger. On the other hand, a larger P_b tends to reduce the above enlarging effect caused by the branching density distribution along the chain. In the case of L4 in which most of the primary chains experience chain transfer reaction, the branching density distribution is found among the primary chains, not along the chain. The g -value is reduced by the branching density distribution in the case, L4.

3.4 Universal g - k Relationship

As shown in Fig. 11 and Fig. 12, it appears that while the g -value for the conventional FRP is significantly smaller than the Zimm-Stockmayer equation, the g -value for the living FRP is rather close to the Zimm-Stockmayer relationship. On the other hand, it is worth noting that the range of the k -values is much different. Even though the average branching density is the same for the corresponding conventional and living FRP, huge polymer molecules are not formed in the living FRP, as shown in the weight fraction distribution, Fig. 9. The branch points are distributed among polymer molecules much more evenly in the living FRP.

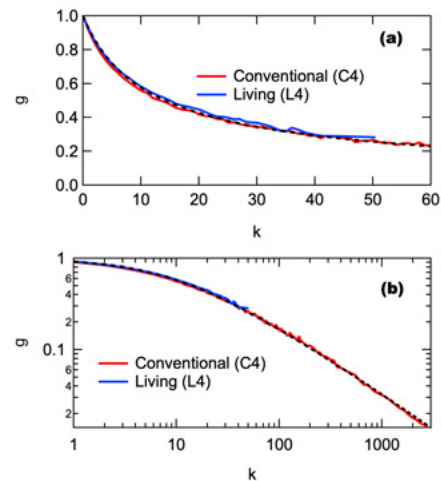


Fig. 14 Universal g - k relationship found for both the conventional and living FRP. (a) Normal plot. (b) Double logarithmic plot.

Fig.14 shows the g - k relationship for C4 and L4, plotted on the same sheet. Both relationships agree well. Note that the g - k relationships of C1–C4 lie on a single curve (Fig. 11), and in addition, L1–L4 agree well (Fig. 12). Therefore, the g - k relationships for all cases can be described by a single universal curve, i.e., the black

dotted curve, which is given by the following empirical equation.

[Emulsion polymerization during Interval II]

$$g = \left[\left(1 + \frac{k}{12} \right)^{0.5} + \frac{k}{5\pi} \right]^{-0.8} \quad (10)$$

The above universal relationship for the emulsion polymerization during Interval II, which is applicable both for the conventional and living FRP, is proposed here.

3.5 Relationship between Rg^2 and the Maximum Span Length, L_{MS}

In a branched polymer molecule, there are many chain ends, as shown in Fig. 15. Within various combination of two chain ends, the longest one is named the maximum span chain, whose length is described as L_{MS} . It is reasonable to consider that L_{MS} has a dominant effect on the mean-square radius of gyration, Rg^2 .

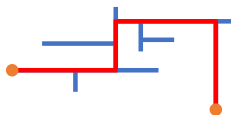


Fig. 15 Schematic representation of the maximum span chain (red), whose length is represented by L_{MS} .

In this article, L_{MS} is represented by the number of monomeric units, and therefore, Rg^2 used here is the one when each monomeric unit is considered as a freely rotating segment. Obviously, a segment consisting of any number of monomeric units can be used, as long as the number of segments is large enough. The above definition (one monomeric unit forms a segment) is needed only for the absolute values of Rg^2 and L_{MS} plotted on the figures.

Fig. 16 shows the Rg^2 - L_{MS} relationship. Each red dot represents a pair of values for each polymer molecule, Rg^2 and L_{MS} . The blue open circles show the average within the intervals of ΔL_{MS} , representing the expected Rg^2 -value for a given L_{MS} . Nice linear relationship is observed.

Fig. 17 shows the expected Rg^2 for the conventional FRPs. All C1–C4 fall nicely on a single line, $Rg^2 = 0.172 L_{MS}$.

Fig. 18 shows the Rg^2 - L_{MS} relationships for the living FRPs. Again, all the relationships for L1–L4 fall on the same line, $Rg^2 = 0.172 L_{MS}$. The relationship, $Rg^2 =$

$0.172 L_{MS}$ applies both for the conventional and living FRP.

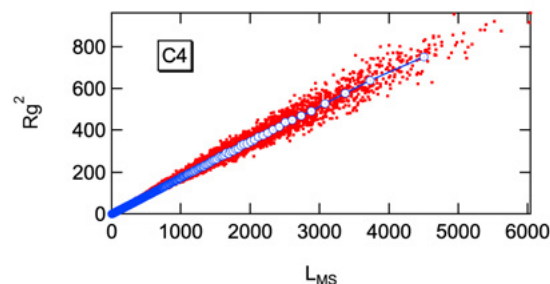


Fig. 16 Relationship between Rg^2 and L_{MS} for the case with C4.

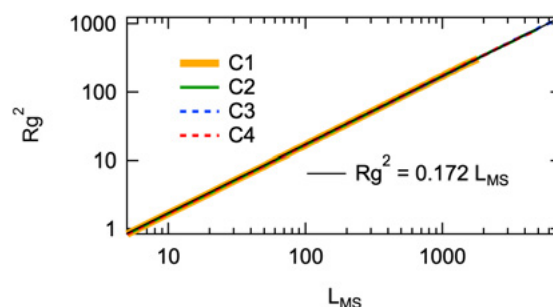


Fig. 17 Relationship between Rg^2 and L_{MS} for the conventional FRP, C1–C4.

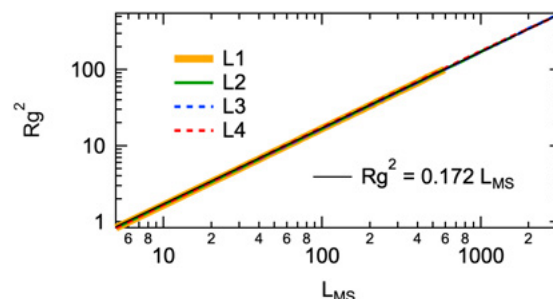


Fig. 18 Rg^2 - L_{MS} relationship for the living FRP, L1–L4.

Essentially the same linear relationship is valid for various types of branched polymers, as summarized in Table 3. The relationship,

$$Rg^2/L_{MS} = 0.17 - 0.18 \quad (11)$$

applies universally for various types of branched polymers that include randomness in their architecture. The value of a is a little larger than $1/6 = 0.167$ for linear polymers, which implies that the polymer chains other than the maximum span chain contribute slightly to increase the a -value.

In order to synthesize branched polymers with large radius of gyration, one should design a branched

architecture whose maximum span length is large. Because L_{MS} is a one-dimensional property, it is much easier than directly imagining complex 3D architectures for the molecular design.

Table 3 Linear relationship $Rg^2 = a L_{MS}$, found for various types of polymers.

Polymer type	a
Emulsion polymerization during Interval II: Conventional FRP with chain transfer to polymer	0.172
Emulsion polymerization during Interval II: Living FRP with chain transfer to polymer	0.172
Random branching of polymer chains ^[10]	0.178
Hyperbranched polymers formed in step polymerization of AB ₂ -type monomer conducted in a batch reactor or in a CSTR ^[11]	0.18
Hyperbranched polymers formed in self-condensing vinyl polymerization (SCVP) conducted in a batch reactor or in a CSTR ^[12]	0.18
Linear polymers ^[9]	0.167
Dendrimer ^[11,12]	0.5

4. Conclusions

The branched architecture formed in the conventional and living emulsion polymerization that involves chain transfer to polymer was investigated theoretically. The simulations were conducted for Interval II, where the polymer/monomer ratio is kept constant.

The MWD formed in the conventional FRP can be very broad, and a bimodal MWD could be formed when the branching probability P_b is large enough. The high MW tail follows the power law, $W(r) \propto r^{-\alpha}$ with $\alpha = 1/P_b$. Controllable power-law distribution can be obtained by using the conventional FRP.

The living FRP leads to form rather narrow MWD. One may overlook the formation of branches, judging solely from the formed MWD.

Both for the conventional and living FRP, the g - k relationship is represented by the following universal relationship [Eq. (10)], which gives smaller g -value compared with the Zimm-Stockmayer formula.

$$g = \left[\left(1 + \frac{k}{12} \right)^{0.5} + \frac{k}{5\pi} \right]^{-0.8}$$

Both for the conventional and living FRP, the

relationship between the mean-square radius of gyration Rg^2 and the maximum span length L_{MS} is represented by $Rg^2 = 0.172 L_{MS}$. For various types of branched polymers, from the polymers with long-chain branches to the hyperbranched polymers synthesized through various types of reaction/reactor, the following simple relationship applies. [Eq. (11)]

$$Rg^2/L_{MS} = 0.17 - 0.18$$

For example, to produce branched polymers having a large radius of gyration, one should think of a production process that leads to give larger values of maximum span length, L_{MS} .

The present work would shed new light on the production technologies for various types of branched polymers with controlled architecture.

References

- [1] H. Tobita: Polym. React. Eng., 1, 357-378 (1993).
- [2] P.J. Flory: Principles of Polymer Chemistry, Cornell University Press, Ithaca, NY, Chap. 9 (1953).
- [3] A.D. Jenkins, R.G. Jones and G. Moad: Pure Appl. Chem., 82, 483-491 (2010).
- [4] H. Tobita: Processes, 6, 14 (2018) [22 pages].
- [5] H. Tobita: Macromol. Theory Simul. 28, 1900018 (2019) [11 pages].
- [6] H. Tobita: e-Polymers, 4, 878-887 (2004).
- [7] H. Tobita: Macromol. Mater. Eng., 290, 363-371 (2005).
- [8] W.H. Starkweather, Jr. and M.C. Han: J. Polym. Sci.: Part A, Polym. Chem., 30, 2709-2713 (1992).
- [9] B.H. Zimm and W.H Stockmayer: J. Chem. Phys., 17, 1301-1314 (1949).
- [10] H. Tobita: Macromol. Theory Simul., 29, 1900057 (2020) [7 pages].
- [11] H. Tobita: Processes, 7, 220 (2019) [18 pages]
- [12] H. Tobita: Macromol. Theory Simul., 28, 1800061 (2019) [10 pages].